

Optimal spin squeezing in cavity-QED-based systems

Vincenzo Macrì,¹ Franco Nori,^{1,2} Salvatore Savasta,^{1,3} and David Zueco^{4,5}

¹ Theoretical Quantum Physics Laboratory, RIKEN Cluster for Pioneering Research, Wako-shi, Saitama 351-0198, Japan

² Physics Department, The University of Michigan, Ann Arbor, Michigan 48109-1040, USA

³ Dipartimento di Scienze Matematiche e Informatiche,

Scienze Fisiche e Scienze della Terra, Università di Messina, I-98166 Messina, Italy

⁴ Instituto de Ciencia de Materiales de Aragón and Departamento de Física de la Materia Condensada ,

CSIC-Universidad de Zaragoza, Pedro Cerbuna 12, 50009 Zaragoza, Spain

⁵ Fundación ARAID, Campus Río Ebro, 50018 Zaragoza, Spain

(Dated: May 1, 2022)

An advantageous architecture for producing deterministic spin squeezing is cavity QED. We show that the recently discovered one photon - two atom excitation process can be used to generate optimal squeezing (scaling as $1/N$) of an ensemble of N spins coupled to a single-mode cavity. This method has some remarkable features. It is a resonant phenomenon mediated by real photons, which provides the advantage of tunability. This allows to create a sizeable squeezing already at the single-photon limit. We show that, close to that resonance, the dynamics can be approximated by a two-axis Hamiltonian. We perform explicit calculations for ensembles of magnetic molecules coupled to a superconducting coplanar cavities obtaining, for realistic parameters, squeezing values up to -30 dB. Thus, this system represents an attractive on-chip architecture for the realization of technological solutions in sensing.

Introduction.— Quantum sensors beat the shot noise limit of precision by using entangled states. Pseudo spin $-1/2$ ensembles, serving as probes for measuring a magnetic field, represent a paradigmatic example [1]. If they are prepared in a convenient squeezed-entangled state, the minimized quadrature reduces the precession angle uncertainty and, thus, the error in the field estimation [2]. The Heisenberg principle imposes the ultimate scaling error as $1/N$, with N the number of spins. Therefore, preparing a macroscopic spin state in a highly squeezed state is a key resource for quantum metrology.

Squeezed states in atomic ensembles are prepared by inducing interactions among the spins. Different schemes, including atom-atom interactions in traps, feedback and projective measurements have shown up to -18 dB quadrature reduction [3–10]. An interesting alternative is the *deterministic* production within one-axis twisting interactions generated inside a cavity [11, 12]. So far, the reported results are limited to -8 dB. Thus, it is desirable to find improved but *deterministic* protocols, as the pre-preparation of initial coherent states superpositions [13]. An alternative is engineering two-axis twisting Hamiltonians that are known to be optimal in the squeezing generation [14, 15]. However, it remains to show their advantage in presence of noise and decoherence [16]. In this work we show how to generate two-axis twisting interactions in spin ensembles coupled to a cavity mode. We show that they are able to generate optimally squeezed states (the squeezing parameter scales as $\xi^2 \sim 1/N$).

The *effective* two-axis twisting interaction proposed here is based on a recent discovered mechanism in cavity QED. In Refs. [17–19] it has been shown that it is possible to excite two atoms simultaneously by absorbing just a single photon between them. The process is reversible, so that the atoms can return to a lower-energy state by

collectively emitting one photon. This is a two-atom resonant process occurring when the atom transition is half of the cavity frequency. Here, we generalize this process to many atoms. This opens the way to investigate cases in which several photons can excite different atomic pairs, producing a coupling interaction in which the square of the global scale spin operators \hat{J}_\pm^2 is involved.

Our protocol differentiates from previous approaches in several ways. Although the light-matter system is in the dispersive regime, it is a resonant mechanism involving *real* photons. This is complementary to the case where the field can be integrated out, so that the spin-spin interactions are mediated by virtual photons [16, 20, 21]. The approach proposed here is a third-order nonlinear optical process boosted by virtual photons [22]. Therefore, for obtaining a significant rate for the excitation of atom pairs, even for weak input fields, the light-atoms coupling rate should reach a significant fraction of the atomic transition frequency. In this interaction regime, known as ultrastrong coupling (USC) [23–25], a generalized theoretical analysis for the output-squeezing should be necessary [26]. However, in this work, the relevant coupling strength is not the single-spin one, g , but the effective *collective interaction* between the N spins and the single-cavity mode, which yields the scaling $\sim g^3 N$. This widely broadens the number of platforms where this process could be implemented. Moreover, it is also required that the atomic or molecular potential does not display inversion symmetry. In this case, the system can be described by an extended Dicke model, with atoms displaying both longitudinal and transverse coupling with the cavity mode (see, e.g., Ref.s [17, 27, 28]). Finally, real photons must be injected inside the cavity. The drive could be even a coherent resonant field. Unexpectedly, we find that even a single cavity photon is able to generate a significant amount of squeezing. A final advantage

of using resonant real photons is that the interaction can be controlled by acting on the driving or on the atoms-cavity detuning.

Our results could be implemented using several kinds of qubits as, e.g., cold atoms, chiral molecules and superconducting flux qubits. One interesting architecture consists of hybrid spin-superconductor systems [29], where the spins can be NV-centers [30–35] or more general spins [36, 37] that are coupled to a superconducting microwave resonator.

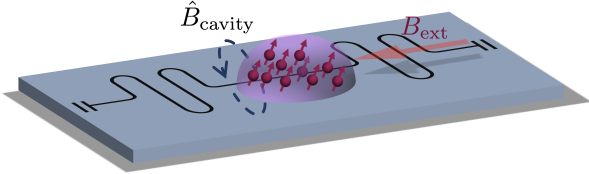


Figure 1. Sketch for the proposed architecture. An ensemble of magnetic molecules (red in the figure) are deposited on top of a superconducting coplanar waveguide resonator. The spin-cavity coupling is mediated by the quantum magnetic field generated by the stationary currents in the circuit, denoted in the figure as \hat{B}_{cavity} . The spins transition frequency can be tuned by means of external control fields, \hat{B}_{ext} .

Resonant excitation of atomic pairs.—Effective Hamiltonian, squeezing parameter.— We consider an ensemble of N identical two level systems equally coupled to a single-mode cavity. The Hamiltonian can be written in terms of collective angular momentum operators:

$$\hat{H} = \frac{\Delta}{2} \hat{J}_z + \frac{\epsilon}{2} \hat{J}_x + \omega_c \hat{a}^\dagger \hat{a} + g(\hat{a} + \hat{a}^\dagger) \hat{J}_x, \quad (1)$$

where $\hat{J}_\alpha = \sum_i \hat{\sigma}_\alpha^i$ ($\alpha = x, y, z$), while \hat{a} and \hat{a}^\dagger are the usual operators for cavity photons. Parity symmetry breaking is described by the second term in Eq. (1). For $\epsilon = 0$ the celebrated Dicke model is recovered [38–41]. When $\epsilon \neq 0$, \hat{H} can couple states differing by an odd number of excitations. For example, an avoided level crossing, originating from the coupling of the states $\hat{a}^\dagger |0, j, -j\rangle \leftrightarrow \hat{J}_+^2 |0, j, -j\rangle$, is expected when the resonance frequency of the cavity $\omega_c \simeq 2\omega_q = 2\sqrt{\Delta^2 + \epsilon^2}$. We label the states as $|n, j, m\rangle$, where the quantum number n describes the Fock states of the cavity, and $j = N/2$ is the total angular momentum and $m = -j + N_{\text{exc}}$ is the \hat{J}_z eigenstate, where N_{exc} describes the number of excited atoms. Such a coupling has been described for the two qubit case ($N = 2$) only in [17]. Figure 2 confirms that it also occurs for any $N \geq 2$. The analysis of those processes non-conserving the number of excitations can be simplified, deriving an effective Hamiltonian by using perturbation theory [42]. For frequencies close to the resonance condition $\omega_c \simeq 2\omega_q$, from Eq. (1), as shown in Appendix A, the following effective interaction Hamiltonian can be obtained:

$$\hat{H}_{\text{eff}} = g_{\text{eff}} \left(\hat{a} \hat{J}_+^2 + \hat{a}^\dagger \hat{J}_-^2 \right), \quad (2)$$

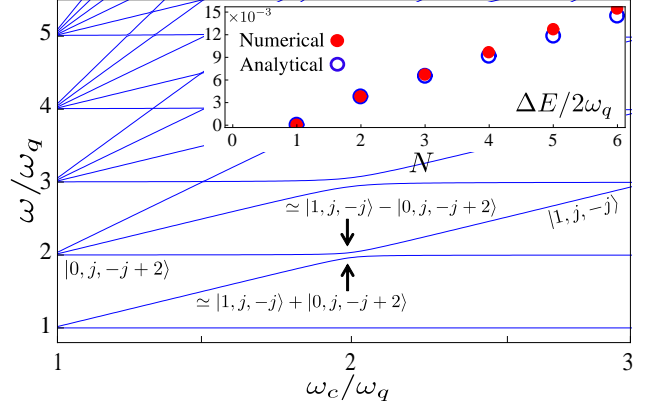


Figure 2. Lowest energy levels of the system Hamiltonian obtained for $N = 20$ qubits versus the ratio between the cavity frequency ω_c and that of identical qubits ω_q . We used $g = 2.5 \times 10^{-4} \omega_q$ and $\theta = \pi/6$. The inset compares the analytical (blue dots) and numerical (red dots) results for the effective coupling between the states $|0, j, -j + 2\rangle$ and $|1, j, -j\rangle$ versus the number of qubits.

where

$$g_{\text{eff}} = -\frac{4g^3 \cos^2 \theta \sin \theta}{3\omega_q^2}, \quad (3)$$

with $\sin \theta = \epsilon / \sqrt{\Delta^2 + \epsilon^2}$. This procedure also gives rise to a renormalization of the atomic frequencies, which can be reabsorbed into ω_q . This effective Hamiltonian yields a series of nonzero transition matrix elements $\langle n-1, j, m+2 | \hat{H}_{\text{eff}} | n, j, m \rangle$, determining a ladder of avoided level crossings at $\omega_c = 2\omega_q$, with energy splittings which are twice these matrix elements. The lowest energy splitting is $\Delta E = 2g_{\text{eff}} \sqrt{2N(N-1)}$. It is worth noticing that, for large N , this splitting scales as $\sim g^3 N$ [see Eq. (3)].

The comparison between $\Delta E/2$ and the corresponding half-splitting energy obtained from the exact numerical diagonalization of the Hamiltonian in Eq. (1) is shown in the inset in Fig. 2. We note the very good agreement. Figure 2 displays the lowest excited energy levels of the effective Hamiltonian (the ground state energy is zero) as a function of ω_c/ω_q , obtained for $N = 20$ qubits. Avoided level crossings are clearly visible at $\omega_c/\omega_q \simeq 2$.

To characterize the squeezing we use the spin-squeezing parameter ξ^2 , proposed by Wineland *et al.* [2, 43, 44],

$$\xi^2 = N \frac{\langle (\hat{\mathbf{J}} \cdot \mathbf{n}_\perp)^2 \rangle - \langle \hat{\mathbf{J}} \cdot \mathbf{n}_\perp \rangle^2}{\langle \hat{\mathbf{J}} \rangle^2}, \quad (4)$$

where the unit vector \mathbf{n}_\perp is chosen to minimize the numerator. This is the ratio between the fluctuations of a general state versus the coherent spin state (CSS), for the determination of the resonance frequency in Ramsey spectroscopy. The CSS here acts as a noise-reference state. For $\xi < 1$ a gain in interferometric precision is possible compared to using a coherent spin state [2, 44].

Single photon squeezing.— The simplest and, at the same time, weirdest illustration of the role of *real* cavity

photons in spin squeezing generation can be obtained by looking at the squeezing generated by a single photon. Let us consider as initial state a superposition of zero and one photon, with all the atoms in their ground state: $|\psi(0)\rangle = \cos\varphi|0, j, -j\rangle + \sin\varphi|1, j, -j\rangle$. Using the effective Hamiltonian in Eq. (2) and neglecting the losses, the time evolution can be analytically calculated:

$$|\psi(t)\rangle = \cos\varphi|0, j, -j\rangle + \sin\varphi \cos(g_{\text{eff}}t)|1, j, -j\rangle - i \sin\varphi \sin(g_{\text{eff}}t)|0, j, -j+2\rangle, \quad (5)$$

from which the spin squeezing parameter in Eq. (4) can be obtained. We chose $\mathbf{n}_\perp = (\cos\phi, \sin\phi, 0)$ (orthogonal to the z axis). In Fig. 3(a) we plot the time evolution of ξ^2 . We also show the mean photon number $\langle\hat{a}^\dagger\hat{a}\rangle = \sin^2\varphi \cos^2(g_{\text{eff}}t)$ and the mean number of excited atoms $N_{\text{exc}} = j + \langle\hat{J}_z\rangle = 2\sin^2\varphi \sin^2(g_{\text{eff}}t)$. We considered a system of $N = 20$ spins with the parameters $g = 0.115\omega_q$, $\theta = \pi/6$ (i.e. $g_{\text{eff}} = 0.01$), and $\varphi = 0.45\pi$. We also used the phase $\phi = \pi/4$, providing the maximum squeezing (corresponding to the minimum value of ξ^2). When the cavity excitation is completely transferred to the ensemble of two-level systems, the squeezing reaches its maximum. This is because the system is in a quantum superposition of the states $|j, -j\rangle$ and $|j, -j+2\rangle$. They are the two first components of an even superposition of coherent states, i.e. an *entangled* cat state. Let us emphasize the maximum amount of quantum-noise reduction obtained, $\xi^2 \simeq 0.55$, already with a single photon. Very similar results can be obtained using the full original Hamiltonian Eq. (1), as reported in Appendix C.

Dissipation and drivings beyond one-photon.— We move to the actual scenario where both the spins and the cavity are affected by dissipation. Assuming that each atom has a γ decay channel, and applying the typical second-order Born and Markov approximations, we end up with the master equation for the density matrix of the cavity plus spins system [see, e.g., [45] and Appendix D]:

$$\dot{\hat{\rho}} = -i[\hat{H}, \hat{\rho}] + \kappa\mathcal{D}[\hat{a}] + \frac{\gamma}{N}\mathcal{D}[\hat{J}_-] \quad (6)$$

where $\mathcal{D}[\hat{O}] = \hat{O}\hat{\rho}\hat{O}^\dagger - 1/2\{\hat{O}^\dagger\hat{O}, \hat{\rho}\}$ are the dissipators in Lindblad form, and κ and γ are the loss rates for the cavity and the spins, respectively. Besides, we extend our discussion to other kinds of drivings. Assuming the system starting in its ground state, we first consider a resonant optical pulse feeding the cavity, including an additional time dependent Hamiltonian term $\hat{V}_d = \mathcal{F}(t)(\hat{a} + \hat{a}^\dagger)$, where $\mathcal{F} = \mathcal{A}\mathcal{G}(t)\cos(\omega_d t)$, with $\mathcal{G}(t)$ being a normalized gaussian function. We consider pulses with central frequency resonant with the cavity ($\omega_d = \omega_c$). Figure 3(b) displays the system dynamics after the pulse arrival, for a system consisting of a cavity mode and $N = 10$ spins. The parameters used are $g = 0.115\omega_q$, $\gamma = 10^{-4}\omega_q$, $\kappa = \gamma/2$, $\mathcal{A}/\omega_q = 3\pi/4$ and $\theta = \pi/6$. The figure shows that the mean photon number $\langle\hat{a}^\dagger\hat{a}\rangle$, as expected, is anticorrelated to the mean

collective spin excitation $j + \langle\hat{J}_z\rangle$. Here, the even spin states superposition involve higher spin states of the type $|j - j + 2n\rangle$, which allows to generate a higher degree of spin squeezing. We also investigate the case of weak continuous driving: $\mathcal{F} = \mathcal{A}\cos(\omega_d t)$ with $\mathcal{A} = 2.5\gamma$. The other parameters used are, $g = 0.115\omega_q$, $\gamma = 10^{-3}\omega_q$ and $\kappa = \gamma$. In Fig. 3(c) we see that squeezing starts to build up when the spin population grows, as expected. In this case, because of the continuous character of the driving, both the cavity and the spins populate to reach a stationary value. The squeezing achieved in these full quantum simulation is quite low, owing to the losses and the low-excitation amplitude.

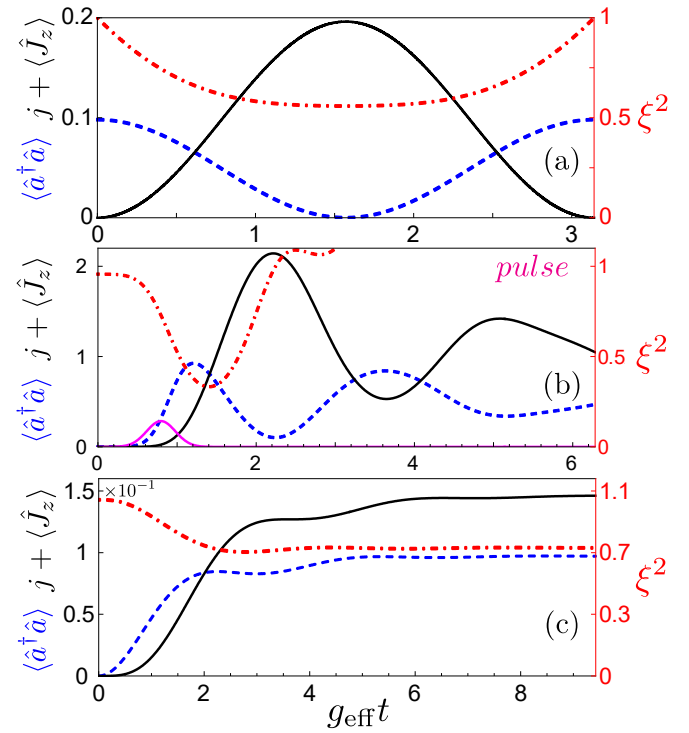


Figure 3. System dynamics for $\omega_c = 2\omega_q$, (a) single-photon dynamics, (b) subject to a π -pulse (magenta solid curve) drive of the cavity mode and (c) under continuous-wave drive of the cavity mode. The blue dashed curve describes the mean photon number $\langle\hat{a}^\dagger\hat{a}\rangle$, while the black solid curve describes the mean collective spin excitation $j + \langle\hat{J}_z\rangle$. The squeezing parameter ξ^2 is also plotted as a red dot-dashed curve with values given on the y axis on the right. All numerical parameters are given in the text.

Macroscopic spin ensemble.— The full quantum numerical simulations are limited to few tens of qubits. However, for most practical purposes $N \gg 1$ is needed. When N is sufficiently large, the collective spin operators can be replaced by a bosonic mode ($\hat{J}_+ \rightarrow \sqrt{N}\hat{b}$), so that the squeezing parameter defined in Eq. (4) tends to the bosonic squeezing measure [2, 46],

$$\xi_{N \rightarrow \infty}^2 = 1 + 2(\langle\hat{b}^\dagger\hat{b}\rangle - |\langle\hat{b}^2\rangle|). \quad (7)$$

In this limit, the effective Hamiltonian [Cf. Eq. (2)] be-

comes

$$\hat{H}_{\text{eff}} = g_{\text{eff}} N (\hat{a} \hat{b}^\dagger + \hat{a}^\dagger \hat{b}^2), \quad (8)$$

while the Lindbladians are replaced consistently: $\frac{1}{N} \mathcal{D}[\hat{J}_-] \rightarrow \mathcal{D}[\hat{b}]$ [Cf. Eq. (6)]. In order to maximize squeezing, a strong driving is required. In this case, a direct simulation in the Fock basis becomes unfeasible, hence we apply the mean-field approximation in order to describe the cavity-spins interaction. In experiments, it is possible to freeze the squeezed state at the time when the maximum squeezing is reached, by detuning the spins transition frequency. Then, the squeezing is preserved for a time determined by the spins decay rate γ . In order to better analyze the squeezing dynamics we derived the equation of motion for the squeezing parameter, in the mean-field approximation

$$\frac{d\xi^2}{dt} = -(i4g_{\text{eff}}N\langle\hat{a}\rangle + \gamma)\xi^2 + \gamma, \quad (9)$$

focusing on its short-time behaviour. In Appendix E, both the bosonic replacement and the mean field approximation have been tested, and the long-time squeezing dynamics is also described. This squeezing evolution is akin to the one arising from the two-axis twisting Hamiltonian, which has been shown to be optimal [2], so that it determines $\xi^2 \sim 1/N$ (in absence of decoherence). Moreover, it squeezes exponentially in time [14, 15]. In previous approaches, based on adiabatic field elimination in the bad-cavity limit, the resulting collective spin decay (induced by the cavity) reduces the degree of squeezing. As a consequence, the resulting spin squeezing scales as $\xi^2 \sim 1/\sqrt{N}$ [2, 7, 16, 21, 47]. In our proposal, the time evolution of the cavity field is taken into account since real photons are involved, and the cavity field, in Eq. (9), may add extra dissipation. However, its effect is negligible if the spins are able to reach the maximum squeezing faster than the cavity dissipation time scale κ^{-1} . We propose a two step protocol. Owing to the resonant nature of the squeezing mechanism studied here, we start setting the spins out of resonance ($\omega_c \neq 2\sqrt{\Delta^2 + \epsilon^2}$) and in their ground state. Then, we drive the cavity by a resonant coherent field, until it reaches $|\langle\hat{a}\rangle| = \sqrt{n_{\text{ph}}}$, where n_{ph} is the steady-state mean photon number in the coherently driven cavity. Once the cavity is fed, the second step starts: the qubits frequency are tuned non-adiabatically into resonance with the cavity. Numerically, taking as initial condition the spins in their ground state and the cavity in a coherent state with $|\langle\hat{a}\rangle| = \sqrt{n_{\text{ph}}}$, we compute the squeezing dynamics within the bosonic replacement. Further details are given in Appendix E. In Fig. 4 we plot our results. They show that the maximum of squeezing is obtained in a time scale

$$(4g_{\text{eff}}N\sqrt{n_{\text{ph}}})^{-1} \equiv (\chi N)^{-1}. \quad (10)$$

Notice that the non-adiabatic tuning of the qubits at the beginning of the second step has to occur within a time much lower than the time-scale in Eq. (10).

The time at which ξ^2 is built up (which marks the short time scale compared to κ and γ within our parameter regime), can be approximately calculated setting $|\langle\hat{a}\rangle| = \sqrt{n_{\text{ph}}}$ (i.e. constant) in Eq. (9). Then, the dynamics can be solved analytically yielding for the squeezing:

$$\xi^2 = \frac{\chi N \exp[-(\chi N + \gamma)t] + \gamma}{\chi N + \gamma}. \quad (11)$$

In Fig. 4(b) we show that this simple formula explains the attainable squeezing (grey solid curves). This approximation works well if $\chi N \gg \kappa$ (see also figure 4(a) and Appendix E). Moreover, the maximum squeezing is obtained if $\chi N \gg \gamma$ is also satisfied. These inequalities are largely satisfied for $\kappa \sim \gamma \sim N g_{\text{eff}}$. Consequently, Eq. (11) shows that ξ^2 is reached exponentially and scales as $1/N$. *This is one of the main results of this letter.*

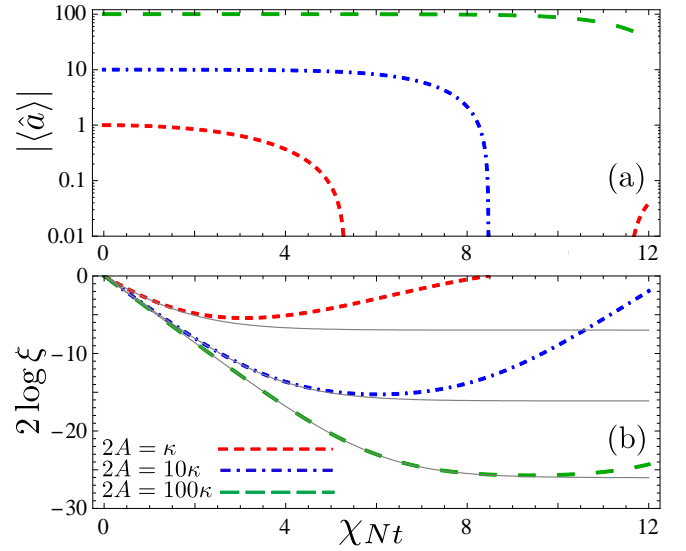


Figure 4. (a) Absolute value of the cavity field coherence $|\langle\hat{a}\rangle|$ versus time, and (b) evolution in dB for the squeezing parameter ξ^2 . Three different values of the drive intensity have been considered: $2A = \kappa, 10\kappa, 100\kappa$ (reported in the legend). The rest of the parameters are $N g_{\text{eff}} = \kappa = \gamma = 1$. The time scale, $(\chi N)^{-1}$ is given by Eq. (10). The solid grey curves describe the results obtained using the analytical result in Eq. (11).

Implementation.— Eq. (11) establishes that ξ^2 decays exponentially to $\gamma/(\chi N)$. This term can be rewritten in terms of both, single qubit-cavity coupling and average number of photons in a driven cavity (n_{ph}) such that $[\gamma/(\chi N)] \sim \gamma [g\sqrt{n_{\text{ph}}}(\sqrt{N}/\omega_q)^2]^{-1}$. Notice that $\sqrt{n_{\text{ph}}} = 2A/\kappa$, where A is the drive amplitude. As said, in the *pros* side is the N^{-1} dependence, together with the enhancement due to the initial driving. However, in the *cons* we have the ratio $(g/\omega_q)^2$. This trade off is better understood by comparing our protocol with similar ones. We consider a recent and optimized protocol [13], which is limited by spins dissipation as $\xi_{\text{Ref.}[12]}^2 \sim \sqrt{\kappa\gamma/Ng^2}$. Writing our scaling in terms

of the latter $\xi^2 \sim (\gamma/\kappa)^{1/2}(\omega_q/g)^2(Nn_{\text{ph}})^{-1/2}\xi_{\text{Ref.}[12]}^2$. Hence, we need to search for architectures where: (i) it is possible to couple a large number of effective spins to a single-mode cavity, (ii) together with a non-negligible single-spin normalized coupling strength (g/ω_q) and (iii) strong cavity pumping is feasible.

Several cavity QED architectures can satisfy the established criteria. Here, we discuss the coupling between single molecular magnets and coplanar waveguide cavities (CPWCs). Using nano-constrictions together with magnetic molecules, single spin-cavity coupling strengths of the order of $g/\omega_q \sim (10^{-4} - 10^{-3})$ can be achieved both for $S = 1/2$ and higher spin molecules having decoherence times up to ms [36, 37]. Moreover, since the molecules are nano-sized objects, a macroscopic number of them can be coupled to the CPWC. In addition, the protocol assumes that turning on and off resonance the spins marks fastest time scale in the problem. Following [37], in our simulations we consider realistic numbers $g/\omega_q \sim 10^{-4}$ and $\gamma \sim \kappa \sim 10^{-5}$. Then, placing $N \sim 10^9$ of those spins we get the parameters used in Fig. 4. Finally, we must consider the maximum power admitted in the nanoconstrictions. Experiments [48] showed that $P_{\text{in}} = -40$ dB (which corresponds to a number of photons $n_{\text{ph}} = 10^{12}$) can be safely used. Setting these realistic parameters we can set $g_{\text{eff}}N = \gamma = \kappa$ obtaining $\xi^2 = -30$ dB as shown in Fig. 4.

Conclusions.— In this letter we have generalized the *one photon-two atom process* in cavity QED to many atoms. In doing so, we have introduced a novel way for generating many-body spin-spin interactions. This yields a two-axis twisting like-interaction among the spins. Note that the mechanism is a resonant process involving real photons which facilitates the control of the effective interaction. We have shown that, already at the single-photon limit, a sizeable squeezing is produced.

Moreover, we showed that by driving strongly the cavity, the scaling for squeezing goes as $\sim 1/N$, corresponding to the Heisenberg limit. We calculated that reaching -30 dB is possible already with spin-cavity and decoherence rates reported for magnetic molecules coupled to superconducting circuit resonators. In addition to this specific platform, our results could be implemented in several cavity QED systems, although the on-chip system analyzed here is particularly advantageous for practical applications. Here, we focused on the squeezing generation; however the novel spin-spin interaction found here can enlarge the possibilities for exploring many body and non linear quantum physics [49]. Finally, we point out that these results show that Dicke-like models can display relevant nonlinear effects in the thermodynamic limit, even under weak coherent optical drives.

Acknowledgments.— DZ acknowledges RIKEN for its hospitality, the support by the Spanish Ministerio de Ciencia, Innovaciòn y Universidades within project MAT2017-88358-C3-1-R. The Aragòn Government project Q-MAD, EU-QUANTERA project SUMO and the Fundaciòn BBVA. FN is supported in part by the: MURI Center for Dynamic Magneto-Optics via the Air Force Office of Scientific Research (AFOSR) (FA9550-14-1-0040), Army Research Office (ARO) (Grant No. W911NF-18-1-0358), Asian Office of Aerospace Research and Development (AOARD) (Grant No.FA2386-18-1-4045), Japan Science and Technology Agency (JST) (via the Q-LEAP program, the ImPACT program, and the CREST Grant No. JPMJCR1676), Japan Society for the Promotion of Science (JSPS) (JSPS-RFBR Grant No. 17-52-50023, and JSPS-FWO Grant No. VS.059.18N), RIKEN-AIST Challenge Research Fund, and the John Templeton Foundation. S.S. acknowledges the Army Research Office (ARO) (Grant No. W911NF1910065).

[1] G. Tóth and I. Apellaniz, “Quantum metrology from a quantum information science perspective,” *J. Phys. A* **47**, 424006 (2014).

[2] J. Ma, X. Wang, C.P. Sun, and F. Nori, “Quantum spin squeezing,” *Phys. Rep.* **509**, 89–165 (2011).

[3] M.F. Riedel, P. Böhi, Y. Li, T. W. Hänsch, A. Sinatra, and P. Treutlein, “Atom-chip-based generation of entanglement for quantum metrology,” *Nature* **464**, 1170 (2010).

[4] D.L. Ian, M. Schleier-Smith, and V. Vladan, “Implementation of Cavity Squeezing of a Collective Atomic Spin,” *Phys. Rev. Lett.* **104**, 073604 (2010).

[5] W. Wasilewski, K. Jensen, H. Krauter, J.J. Renema, M.V. Balabas, and E.S. Polzik, “Quantum Noise Limited and Entanglement-Assisted Magnetometry,” *Phys. Rev. Lett.* **104**, 133601 (2010).

[6] W. Muessel, H. Strobel, D. Linnemann, D.B. Hume, and M.K. Oberthaler, “Scalable Spin Squeezing for Quantum-Enhanced Magnetometry with Bose-Einstein Condensates,” *Phys. Rev. Lett.* **113**, 103004 (2014).

[7] M. Schleier-Smith, D.L. Ian, and V. Vladan, “States of an Ensemble of Two-Level Atoms with Reduced Quantum Uncertainty,” *Phys. Rev. Lett.* **104**, 073604 (2010).

[8] J.G. Bohnet, K.C. Cox, M.A. Norcia, J. M. Weiner, Z. Chen, and J. K. Thompson, “Reduced spin measurement back-action for a phase sensitivity ten times beyond the standard quantum limit,” *Nat. Photonics* **8**, 731–736 (2014).

[9] G. Vasilakis, H. Shen, K. Jensen, M. Balabas, D. Salart, B. Chen, and E.S. Polzik, “Generation of a squeezed state of an oscillator by stroboscopic back-action-evading measurement,” *Nat. Phys.* **11**, 389–392 (2015).

[10] O. Hosten, R. Krishnakumar, N.J. Engelsen, and M.A. Kasevich, “Quantum phase magnification,” *Science* **352**, 1552–1555 (2016).

[11] O. Hosten, N.J. Engelsen, R. Krishnakumar, and M.A. Kasevich, “Measurement noise 100 times lower than the quantum-projection limit using entangled atoms,” *Nature* **529**, 505–508 (2016).

[12] M.A. Norcia, R.J. Lewis-Swan, J.R.K. Cline, B. Zhu,

A.M. Rey, and J.K. Thompson, “Cavity-mediated collective spin-exchange interactions in a strontium superradiant laser,” *Science* **361**, 259–262 (2018).

[13] R.J. Lewis-Swan, M.A. Norcia, J.R. Cline, J.K. Thompson, and A.M. Rey, “Robust Spin Squeezing via Photon-Mediated Interactions on an Optical Clock Transition,” *Phys. Rev. Lett.* **121**, 070403 (2018).

[14] T. Opatrný, “Twisting tensor and spin squeezing,” *Phys. Rev. A* **91**, 053826 (2015).

[15] Y.C. Liu, Z.F. Xu, G.R. Jin, and L. You, “Spin Squeezing: Transforming One-Axis Twisting into Two-Axis Twisting,” *Phys. Rev. Lett.* **107**, 013601 (2011).

[16] J. Borregaard, E.J. Davis, G.S. Bentsen, M.H. Schleier-Smith, and A.S. Sørensen, “One- and two-axis squeezing of atomic ensembles in optical cavities,” *New J. Phys.* **19**, 093021 (2017).

[17] L. Garziano, V. Macrì, R. Stassi, O. Di Stefano, F. Nori, and S. Savasta, “One Photon Can Simultaneously Excite Two or More Atoms,” *Phys. Rev. Lett.* **117**, 043601 (2016).

[18] P. Zhao, X. Tan, H. Yu, S.L. Zhu, and Y. Yu, “Simultaneously exciting two atoms with photon-mediated Raman interactions,” *Phys. Rev. A* **95**, 063848 (2017).

[19] X. Wang, A. Miranowicz, H.R. Li, and F. Nori, “Observing pure effects of counter-rotating terms without ultrastrong coupling: A single photon can simultaneously excite two qubits,” *Phys. Rev. A* **96**, 063820 (2017).

[20] G. Agarwal, R. Puri, and R. Singh, “Atomic Schrödinger cat states,” *Phys. Rev. A* **56**, 2249–2254 (1997).

[21] A.S. Sørensen and K. Mølmer, “Entangling atoms in bad cavities,” *Phys. Rev. A* **66**, 022314 (2002).

[22] A. F. Kockum, A. Miranowicz, V. Macrì, and F. Savasta, S. and Nori, “Deterministic quantum nonlinear optics with single atoms and virtual photons,” *Phys. Rev. A* **95**, 063849 (2017).

[23] T. Niemczyk, F. Deppe, H. Huebl, E.P. Menzel, F. Hocke, M.J. Schwarz, J.J. García-Ripoll, D. Zueco, T. Hümmer, E. Solano, A. Marx, and R. Gross, “Circuit quantum electrodynamics in the ultrastrong-coupling regime,” *Nat. Phys.* **6**, 772–776 (2010).

[24] A.F. Kockum, A. Miranowicz, S. De Liberato, S. Savasta, and F. Nori, “Ultrastrong coupling between light and matter,” *Nat. Rev. Phys.* **1**, 19 (2019).

[25] P. Forn-Díaz, L. Lamata, E. Rico, J. Kono, and E. Solano, “Ultrastrong coupling regimes of light-matter interaction,” [arXiv:1804.09275](https://arxiv.org/abs/1804.09275) (2018).

[26] R. Stassi, S. Savasta, Luigi G., B. Spagnolo, and F. Nori, “Output field-quadrature measurements and squeezing in ultrastrong cavity-QED,” *New J. Phys.* **18**, 123005 (2016).

[27] L. Garziano, V. Stassi, R. and Macrì, A.F. Kockum, S. Savasta, and F. Nori, “Multiphoton quantum Rabi oscillations in ultrastrong cavity QED,” *Phys. Rev. A* **92**, 063830 (2015).

[28] N. Lambert, M. Cirio, M. Delbecq, G. Allison, M. Marx, S. Tarucha, and F. Nori, “Amplified and tunable transverse and longitudinal spin-photon coupling in hybrid circuit-QED,” *Phys. Rev. B* **97**, 125429 (2018).

[29] Ze-Liang Xiang *et al.*, “Hybrid quantum circuits: Superconducting circuits interacting with other quantum systems,” *Rev. Mod. Phys.* **85**, 623–653 (2013).

[30] D.I. Schuster, A.P. Sears, E. Ginossar, L. DiCarlo, L. Frunzio, J.J.L. Morton, H. Wu, G.A.D. Briggs, B.B. Buckley, D.D. Awschalom, and R.J. Schoelkopf, “High- Cooperativity Coupling of Electron-Spin Ensembles to Superconducting Cavities,” *Phys. Rev. Lett.* **105**, 140501 (2010).

[31] Y. Kubo, F.R. Ong, P. Bertet, D. Vion, V. Jacques, D. Zheng, A. Dréau, J.F. Roch, A. Auffeves, F. Jelezko, J. Wrachtrup, M.F. Barthe, P. Bergonzo, and D. Esteve, “Strong Coupling of a Spin Ensemble to a Superconducting Resonator,” *Phys. Rev. Lett.* **105**, 140502 (2010).

[32] H. Wu, R.E. George, J.H. Wesenberg, K. Mølmer, D.I. Schuster, R.J. Schoelkopf, K.M. Itoh, A. Ardavan, J.J.L. Morton, and G.A.D. Briggs, “Storage of Multiple Coherent Microwave Excitations in an Electron Spin Ensemble,” *Phys. Rev. Lett.* **105**, 140503 (2010).

[33] R. Amsüss, C. Koller, T. Nöbauer, S. Putz, S. Rotter, K. Sandner, S. Schneider, M. Schramböck, G. Steinhäuser, H. Ritsch, J. Schmiedmayer, and J. Majer, “Cavity QED with Magnetically Coupled Collective Spin States,” *Phys. Rev. Lett.* **107**, 060502 (2011).

[34] Xin-You Lü *et al.*, “Quantum memory using a hybrid circuit with flux qubits and nitrogen-vacancy centers,” *Phys. Rev. A* **88**, 012329 (2013).

[35] Ze-Liang Xiang *et al.*, “Hybrid quantum circuit consisting of a superconducting flux qubit coupled to a spin ensemble and a transmission-line resonator,” *Phys. Rev. B* **87**, 144516 (2013).

[36] M. Jenkins, T. Hümmer, M.J. Martínez-Pérez, J. García-Ripoll, D. Zueco, and F. Luis, “Coupling single-molecule magnets to quantum circuits,” *New. J. Phys.* **15**, 095007 (2013).

[37] M.D. Jenkins, D. Zueco, O. Roubeau, G. Aromí, J. Majer, and F. Luis, “A scalable architecture for quantum computation with molecular nanomagnets,” *Dalton Trans.* **45**, 16682–16693 (2016).

[38] B.M. Garraway, “The Dicke model in quantum optics: Dicke model revisited,” *Philos. Trans. Royal Soc. A* **369**, 1137–1155 (2011).

[39] N. Shammah, N. Lambert, F. Nori, and S. De Liberato, “Superradiance with local phase-breaking effects,” *Phys. Rev. A* **96**, 023863 (2017).

[40] N. Shammah, S. Ahmed, N. Lambert, S. De Liberato, and F. Nori, “Open quantum systems with local and collective incoherent processes: Efficient numerical simulations using permutational invariance,” *Phys. Rev. A* **98**, 063815 (2018).

[41] P. Kirton, M.M. Roses, J. Keeling, and E.G. Dalla Torre, “Introduction to the Dicke model: from equilibrium to nonequilibrium, and vice versa,” [arXiv:1805.09828](https://arxiv.org/abs/1805.09828) (2018).

[42] W. Shao, C. Wu, and X.L. Feng, “Generalized James’ effective Hamiltonian method,” *Phys. Rev. A* **95**, 032124 (2017).

[43] D.J. Wineland, J.J. Bollinger, W.M. Itano, F.L. Moore, and D.J. Heinzen, “Spin squeezing and reduced quantum noise in spectroscopy,” *Phys. Rev. A* **46**, R6797–R6800 (1992).

[44] D.J. Wineland, J.J. Bollinger, W.M. Itano, and D.J. Heinzen, “Squeezed atomic states and projection noise in spectroscopy,” *Phys. Rev. A* **50**, 67–88 (1994).

[45] J. Gelhausen, M. Buchhold, and P. Strack, “Many-body quantum optics with decaying atomic spin states: (γ, κ) Dicke model,” *Phys. Rev. A* **95**, 063824 (2017).

[46] X. Wang and B.C. Sanders, “Relations between bosonic quadrature squeezing and atomic spin squeezing,” *Phys. Rev. A* **68**, 033821 (2003).

[47] E.G. Dalla Torre, J. Otterbach, E. Demler, V. Vuletic, and M.D. Lukin, “Dissipative Preparation of Spin Squeezed Atomic Ensembles in a Steady State,” *Phys. Rev. Lett.* **110**, 120402 (2013).

[48] M.D. Jenkins, U. Naether, M. Ciria, J. Sesé, J. Atkinson, C. Sánchez-Azqueta, E. Del Barco, J. Majer, D. Zueco, and F. Luis, “Nanoscale constrictions in superconducting coplanar waveguide resonators,” *Appl. Phys. Lett.* **105**, 162601 (2014).

[49] V. Stassi, R. and Macrì, A.F. Kockum, O. Di Stefano, A. Miranowicz, S. Savasta, and F. Nori, “Quantum nonlinear optics without photons,” *Phys. Rev. A* **96**, 023818 (2017).

[50] Liu Yu xi *et al.*, “Optical Selection Rules and Phase-Dependent Adiabatic State Control in a Superconducting Quantum Circuit,” *Phys. Rev. Lett.* **95**, 087001 (2005).

[51] T. Hümmer, G. M. Reuther, P. Hänggi, and D. Zueco, “Nonequilibrium phases in hybrid arrays with flux qubits and nitrogen-vacancy centers,” *Phys. Rev. A* **85**, 052320 (2012).

Appendix A: Two-level atoms: Derivation of the effective Hamiltonian

In order to derive the effective Hamiltonian in Eq. (2) (see the main text), we start from Eq. (1). We first rewrite it in the basis where the qubits Hamiltonian (in the presence of interaction) is diagonal. We obtain

$$\hat{H} = \omega_q \hat{J}_z + \omega_c \hat{a}^\dagger \hat{a} + g(\hat{a} + \hat{a}^\dagger)(\cos \theta \hat{J}_x + 2 \sin \theta \hat{J}_z), \quad (\text{A1})$$

where

$$2\hat{J}_z = \sum_i \hat{\sigma}_z^{(i)}. \quad (\text{A2})$$

Notice that the flux offset, is now encoded in the angle $\theta = \arctan(\epsilon/\Delta)$. We now apply the generalized James’ effective Hamiltonian method [42]. In the interaction picture, the system Hamiltonian in Eq. (A1) contains terms with three distinct frequencies. For $\omega_c = 2\omega_q$,

the three frequencies are $\omega_1 = \omega_q$, $\omega_2 = 2\omega_q$, and $\omega_3 = 3\omega_q$. The terms are

$$\begin{aligned} \hat{h}_1 &= g \cos \theta \hat{a}^\dagger \sum_i \hat{\sigma}_-^i \\ \hat{h}_2 &= -g \sin \theta \hat{a}^\dagger \sum_i \hat{\sigma}_z^i \\ \hat{h}_3 &= g \cos \theta \hat{a}^\dagger \sum_i \hat{\sigma}_+^i. \end{aligned} \quad (\text{A3})$$

The light-matter interaction potential can then be written as

$$\hat{V} = \sum_{i=1}^3 \hat{h}_i + \text{H.c.} \quad (\text{A4})$$

By applying the generalized James’ method [Eq. (15) of Ref. [42]] and neglecting the time dependent terms (RWA), we obtain the effective Hamiltonian:

$$\begin{aligned} \hat{H}_{\text{eff}} = & -A \left[\hat{h}_1 \hat{h}_2^\dagger \hat{h}_1 + \hat{h}_1^\dagger \hat{h}_2 \hat{h}_1^\dagger \right] \\ & + \frac{A}{2} \left[\hat{h}_1 \hat{h}_1 \hat{h}_2^\dagger + \hat{h}_1^\dagger \hat{h}_1^\dagger \hat{h}_2 + \hat{h}_2^\dagger \hat{h}_1 \hat{h}_1 + \hat{h}_2 \hat{h}_1^\dagger \hat{h}_1^\dagger \right] \\ & - \frac{A}{2} \left[\hat{h}_1 \hat{h}_3^\dagger \hat{h}_2 + \hat{h}_2 \hat{h}_3^\dagger \hat{h}_1 + \hat{h}_2^\dagger \hat{h}_3 \hat{h}_1^\dagger + \hat{h}_1^\dagger \hat{h}_3 \hat{h}_2^\dagger \right] \\ & + \frac{A}{3} \left[\hat{h}_1 \hat{h}_2 \hat{h}_3^\dagger + \hat{h}_1^\dagger \hat{h}_2^\dagger \hat{h}_3 + \hat{h}_3^\dagger \hat{h}_2 \hat{h}_1 + \hat{h}_3 \hat{h}_2^\dagger \hat{h}_1^\dagger \right] \\ & + \frac{A}{6} \left[\hat{h}_2 \hat{h}_1 \hat{h}_3^\dagger + \hat{h}_2^\dagger \hat{h}_1^\dagger \hat{h}_3 + \hat{h}_3^\dagger \hat{h}_1 \hat{h}_2 + \hat{h}_3 \hat{h}_1^\dagger \hat{h}_2^\dagger \right], \end{aligned} \quad (\text{A5})$$

where $A = g^3 \cos^2 \theta \sin \theta / \omega_q^2$. Adopting normal ordering for the photonic operators, neglecting higher-order terms involving two destruction or creation photon operators, and using the commutation rules for the Pauli operators, Eq. (A5) becomes:

$$\begin{aligned} \hat{H}_{\text{eff}} = & -2A \left[\hat{a} \sum_{jk} \hat{\sigma}_+^j \hat{\sigma}_+^k + \hat{a}^\dagger \sum_{jk} \hat{\sigma}_-^j \hat{\sigma}_-^k \right] - \frac{A}{2} \left[2\hat{a} \sum_{ijk} \hat{\sigma}_+^j \hat{\sigma}_+^k \hat{\sigma}_z^i + 4\hat{a} \sum_{jk} \hat{\sigma}_+^j \hat{\sigma}_+^k + 2\hat{a} \sum_{ijk} \hat{\sigma}_-^j \hat{\sigma}_-^k \hat{\sigma}_z^i - 4\hat{a} \sum_{jk} \hat{\sigma}_-^j \hat{\sigma}_-^k \right] \\ & + \frac{2A}{3} \left[\hat{a} \sum_{ijk} \hat{\sigma}_+^j \hat{\sigma}_+^k \hat{\sigma}_z^i + 2\hat{a} \sum_{jk} \hat{\sigma}_+^j \hat{\sigma}_+^k + \hat{a} \sum_{ijk} \hat{\sigma}_-^j \hat{\sigma}_-^k \hat{\sigma}_z^i - 2\hat{a} \sum_{jk} \hat{\sigma}_-^j \hat{\sigma}_-^k \right] \\ & + \frac{A}{3} \left[\hat{a} \sum_{ijk} \hat{\sigma}_+^j \hat{\sigma}_+^k \hat{\sigma}_z^i + 4\hat{a} \sum_{jk} \hat{\sigma}_+^j \hat{\sigma}_+^k + \hat{a} \sum_{ijk} \hat{\sigma}_-^j \hat{\sigma}_-^k \hat{\sigma}_z^i \right]. \end{aligned} \quad (\text{A6})$$

After some algebra, we obtain the effective Hamiltonian:

$$\hat{H}_{\text{eff}} = -\frac{4g^3 \cos^2 \theta \sin \theta}{3\omega_q^2} \left(\hat{a} \sum_{jk} \hat{\sigma}_+^j \hat{\sigma}_+^k + \hat{a}^\dagger \sum_{jk} \hat{\sigma}_-^j \hat{\sigma}_-^k \right). \quad (\text{A7})$$

We note that the the resulting effective Hamiltonian does not depend on the Pauli operator $\hat{\sigma}_z$. Using the collective lowering and raising spin operators Eq. (A2), becomes:

$$\hat{H}_{\text{eff}} = -\frac{4g^3 \cos^2 \theta \sin \theta}{3\omega_q^2} \left(\hat{a} \hat{J}_+^2 + \hat{a}^\dagger \hat{J}_-^2 \right). \quad (\text{A8})$$

Here $J_\pm = \sum_j \sigma_\pm$. Equation (A8) displays the effective Hamiltonian, describing the simultaneous generation of two excitations in an ensamble constituted by an arbitrary number N of identical atoms, by one photon absorption. Equation (A8) is the effective Hamiltonian responsible for the coupling between the eigenvectors $|0, ggg..e..e..ggg..\rangle$ and $|1, ggg..g..g..ggg..\rangle$. In terms of the angular momentum notation, they can be written as $|0, j, -j+2\rangle$ and $|1, j, -j\rangle$, respectively, being $j = N/2$. More generally, this Hamiltonian couples states differing by two-qubit excitations: $|j, m\rangle \leftrightarrow |j, m+2\rangle$. The effective resonant coupling between these eigenstates, for $m = -j$ is:

$$\langle 0, j, -j+2 | H_{\text{eff}} | 1, j, -j \rangle = \frac{4g^3 \cos^2 \theta \sin \theta}{3\omega_q^2} \sqrt{2N(N-1)}. \quad (\text{A9})$$

Appendix B: Δ -like three-level atoms: Derivation of the effective Hamiltonian

It has been shown [18] that it is possible to simultaneously excite two atoms by using a cavity-assisted Raman process in combination with a cavity-photon-mediated interaction. We generalize this analysis to a system of many atoms.

Specifically, we consider a system of N Δ -like three-level atoms interacting with a single mode optical resonator [18, 50]. The total Hamiltonian is $\hat{H}_\Delta = \hat{H}_c + \hat{H}_0 + \hat{V}_I$, being

$$\hat{H}_c = \omega_c \hat{a}^\dagger \hat{a}, \quad (\text{B1})$$

the energy of the cavity,

$$\hat{H}_0 = \sum_i \left(\omega_g \hat{\sigma}_{gg}^{(i)} + \omega_e \hat{\sigma}_{ee}^{(i)} + \omega_s \hat{\sigma}_{ss}^{(i)} \right), \quad (\text{B2})$$

the energy of an ensemble of identical three-level (g, e, s) atoms (here, $\hat{\sigma}_{mn}^{(i)} = |m\rangle_i \langle n|$, where $|m\rangle_i$ is a generic eigenstate of the three-level atom with $m, n = g, e, s$), and finally,

$$\hat{V}_I = \hat{a} \sum_{i=1}^N \left(g_{ge} \hat{\sigma}_{eg}^{(i)} + g_{gs} \hat{\sigma}_{sg}^{(i)} + g_{es} \hat{\sigma}_{se}^{(i)} \right) + \text{H.c.} \quad (\text{B3})$$

is the interaction Hamiltonian part. The term $\hat{\sigma}_{mn}^{(i)} = |m\rangle \langle n|$ is a transition operator for the i -th three-level atom, while g_{mn} is the corresponding transition matrix elements. Assuming that the system operates in the dispersive regime: $|\Delta_{mn}| \gg g_{nm}$, where $\Delta_{mn} = \omega_{mn} - \omega_c$ and $\omega_{mn} = \omega_m - \omega_n$ denote the transition frequencies, it is possible to derive the effective Hamiltonian applying a unitary transformation able to eliminate the direct atom-cavity coupling:

$$\hat{H}_{\text{eff}} = e^{-\hat{X}} \hat{H}_\Delta e^{\hat{X}}, \quad (\text{B4})$$

where

$$\hat{X} = \sum_{i=1}^N \left(\frac{g_{ge}}{\Delta_{eg}} \hat{\sigma}_{eg}^{(i)} + \frac{g_{es}}{\Delta_{se}} \hat{\sigma}_{se}^{(i)} + \frac{g_{gs}}{\Delta_{sg}} \hat{\sigma}_{sg}^{(i)} - \text{H.c.} \right). \quad (\text{B5})$$

Keeping terms up to the third order in the interaction Hamiltonian, assuming that no atom is initially in the $|s\rangle$ state, assuming $\omega_c \simeq 2\omega_{eg}$, and including only the time-independent terms (in the Heisenberg picture), we obtain the effective Hamiltonian

$$\hat{H}_{\text{eff}} = g_{\text{eff}} \left(\hat{a} \hat{J}_+^2 + \hat{a}^\dagger \hat{J}_-^2 \right), \quad (\text{B6})$$

with the resulting effective coupling strength

$$g_{\text{eff}} = \frac{g_{ge} g_{gs} g_{se}}{3\Delta_{ig} \Delta_{ie} \Delta_{eg}} (3\Delta_{ig} - \omega_{eg}). \quad (\text{B7})$$

Notice that in Eq. (B6) $\hat{J}_+ = \sum_i \hat{\sigma}_{eg}^{(i)}$.

Appendix C: System dynamics using the Hamiltonian in Eq. (1)

Here we compare the analytically calculated system dynamics [see Fig. 3(a)], obtained by using the effective Hamiltonian in Eq. (2), with the dynamics calculated numerically by using the full system Hamiltonian in Eq. (A1) (which is equivalent to Eq. (1)). We analyze the free system evolution, considering as initial condition a superposition state of the system ground state and a one-photon state with all the spins in their ground state (see the main paper). All the parameters used here coincide with those used to obtain the results in Fig. 3(a).

Figure (5) displays such a comparison. Specifically, the continuous curves describe the mean number of cavity photons (blue) as well as the mean excitation number for the spin system (black), and the squeezing parameter (red) obtained using Eq. (1) (numerical calculation). The dashed curves correspond to the analytical calculations displayed in Fig. 3(a). The agreement between the

two set of curves is very good, showing that the effective Hamiltonian is able to describe well this interacting system under the resonant condition $\omega_c \simeq 2\omega_q$, at least for a moderate light-matter interaction strength.

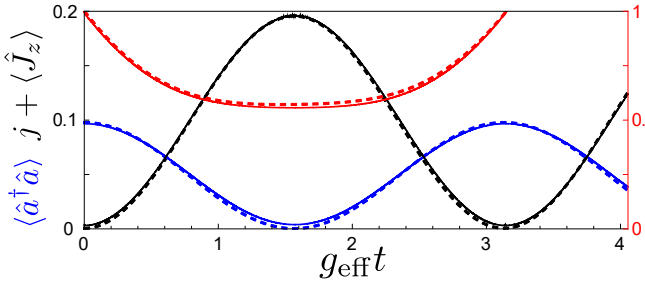


Figure 5. Free time evolution of the interacting light matter system, considering $N = 10$ effective spins for $\omega_c = 2\omega_q$. The initial state is a superposition of the system ground state and a one-photon state with all the spins in their ground state (see the main paper). The continuous curves describe the mean number of cavity photons (blue) as well as the mean excitation number for the spin system (black), and the squeezing parameter (red) obtained using Eq. (1) (numerical calculation). The dashed curves do corresponds to the analytical results displayed in Fig. 3(a).

Appendix D: Dissipation

The Linblad dissipators for a collection of two level systems inside a cavity have been discussed in Ref. [45]. In this appendix we develop a similar theory adapting it to our case. We assume that the ensemble of spins occupies a small volume, compared to the cavity-mode wavelength. This is the case for the implementation discussed in the main text. With this assumption, both the cavity and atomic decays can be cast in the Lindblad form [45]:

$$\kappa \mathcal{D}[\hat{a}] = \kappa (2\hat{a}\hat{\varrho}\hat{a}^\dagger - \{\hat{a}^\dagger\hat{a}, \hat{\varrho}\}), \quad (D1)$$

$$\gamma \mathcal{D}[\hat{\sigma}] = \gamma \sum_i \hat{\sigma}_-^i \hat{\varrho} \hat{\sigma}_+^i - \frac{1}{2} \{\hat{\sigma}_+^i \hat{\sigma}_-^i, \hat{\varrho}\} \quad (D2)$$

Here, γ and κ are the atomic and cavity decay rates, respectively. Taking the Fourier transform,

$$\hat{\sigma}_+^k = \frac{1}{\sqrt{N}} \sum_j e^{ikj} \hat{\sigma}_j^k \quad (D3)$$

we notice that

$$\hat{\sigma}_\pm^0 = \frac{1}{\sqrt{N}} \hat{J}_\pm. \quad (D4)$$

Using Eq. (D3), the single-site dissipative terms becomes:

$$\begin{aligned} \sum_i \hat{\sigma}_-^i \hat{\varrho} \hat{\sigma}_+^i - \frac{1}{2} \{\hat{\sigma}_+^i \hat{\sigma}_-^i, \hat{\varrho}\} \\ = \frac{1}{N} \sum_{k, k'} \sum_j e^{i(k-k')j} \left(\hat{\sigma}_-^k \hat{\varrho} \hat{\sigma}_+^{k'} - \frac{1}{2} \{\hat{\sigma}_+^{k'} \hat{\sigma}_-^k, \hat{\varrho}\} \right), \end{aligned} \quad (D5)$$

It is convenient to separate the zero momentum contribution, which, using Eq. (D4), results into:

$$\begin{aligned} \gamma \mathcal{D}[\hat{\sigma}] = & \frac{\gamma}{N} (\hat{J}_- \hat{\varrho} \hat{J}_+ - \frac{1}{2} \{\hat{J}_+ \hat{J}_-, \hat{\varrho}\}) \\ & + \gamma \sum_{k \neq 0} \hat{\sigma}_-^k \hat{\varrho} \hat{\sigma}_+^k - \frac{1}{2} \{\hat{\sigma}_+^k \hat{\sigma}_-^k, \hat{\varrho}\}. \end{aligned} \quad (D6)$$

Finally, we analize how the terms in the Hamiltonian (1) looks like in momentum space. For that, we realize that [Cf. Eq. (D5)]:

$$\sum_i \hat{\sigma}_+^i \hat{\sigma}_-^i = \sum_k \hat{\sigma}_+^k \hat{\sigma}_-^k. \quad (D7)$$

Moreover, the atomic-light coupling becomes:

$$g(\hat{a} + \hat{a}^\dagger) \sum_i \hat{\sigma}_x^i = g(\hat{a} + \hat{a}^\dagger)(\hat{J}_+ + \hat{J}_-) \quad (D8)$$

As expected, the cavity only couples to the zero momentum operator. Therefore, the full dynamics (unitary + dissipative) do not mix different momenta, resulting in the QME used in the main text.

Appendix E: Bosonic map in the large- N limit

If N is sufficiently large and the number of spin excitations satisfies the condition $\sum_j \langle \hat{\sigma}_j^+ \hat{\sigma}_j^- \rangle \ll N$, the collective spin operator can be replaced [51] by a bosonic mode:

$$\hat{J}_- \equiv \sum_i \hat{\sigma}_-^{(i)} \rightarrow \sqrt{N} \hat{b}, \quad (E1)$$

$$\hat{J}_+ \equiv \sum_i \hat{\sigma}_+^{(i)} \rightarrow \sqrt{N} \hat{b}^\dagger, \quad (E2)$$

where \hat{b} (\hat{b}^\dagger) is the creation (destruction) operator in the new bosonic rappresentation. Using Eq. (E1), Eq. (E2) and including a continuum driving term $2A \cos(\omega_d t)(\hat{a} + \hat{a}^\dagger)$ (in the rotating wave approximation), the system Hamiltonian in the rotating frame becomes:

$$\hat{H} = (\omega_c - \omega_d) \hat{a}^\dagger \hat{a} + \omega_q \hat{b}^\dagger \hat{b} + g_{\text{eff}} N (\hat{a} \hat{b}^\dagger)^2 + \hat{a}^\dagger \hat{b}^2 + A(\hat{a} + \hat{a}^\dagger). \quad (E3)$$

Notice that, since $\langle \hat{b}^\dagger \rangle^2 |0\rangle = \sqrt{2} |2\rangle$, the anticrossing scales as $\sqrt{2} N$ which equals $\sqrt{2N(N-1)}$, in the $N \rightarrow \infty$ limit [Cf. Eq. (3) in the main text].

As regards the dissipators, they are global spin operators (see Appendix D). Thus, after the replacement by a bosonic mode the master equation becomes

$$\begin{aligned} \dot{\hat{\varrho}} = & -i[\hat{H}_{\text{bosonic}}, \hat{\varrho}] \\ & + \kappa (2\hat{a}\hat{\varrho}\hat{a}^\dagger - \{\hat{a}^\dagger\hat{a}, \hat{\varrho}\}) + \gamma (\hat{b}\hat{\varrho}\hat{b}^\dagger - \frac{1}{2} \{\hat{b}^\dagger\hat{b}, \hat{\varrho}\}) \end{aligned} \quad (E4)$$

Due to the nonlinearity of the system Hamiltonian, Eq. (E4) is not exactly solvable. Applying the mean-field approximation $\langle \hat{a}\hat{b}^\dagger \rangle \rightarrow \langle \hat{a} \rangle \langle \hat{b}^\dagger \rangle$, with the purpose

to describe the cavity-spins interaction, we end up with a non-linear and closed set of coupled equations for the first and second moments:

$$\partial_t \langle \hat{a} \rangle = -iN g_{\text{eff}} \langle \hat{b}^2 \rangle - iA - \frac{\kappa}{2} \langle \hat{a} \rangle \quad (\text{E5a})$$

$$\partial_t \langle \hat{b} \rangle = -iN g_{\text{eff}} \langle \hat{a} \rangle \langle \hat{b}^\dagger \rangle - \frac{\gamma}{2} \langle \hat{b} \rangle \quad (\text{E5b})$$

$$\partial_t \langle \hat{b}^2 \rangle = -i2N g_{\text{eff}} \langle \hat{a} \rangle (2\langle \hat{b}^\dagger \hat{b} \rangle + 1) - \gamma \langle \hat{b}^2 \rangle \quad (\text{E5c})$$

$$\partial_t \langle \hat{b}^\dagger \hat{b} \rangle = -i2N g_{\text{eff}} (\langle \hat{a} \rangle \langle \hat{b}^\dagger \rangle^2 - \text{c.c.}) - \gamma \langle \hat{b}^\dagger \hat{b} \rangle. \quad (\text{E5d})$$

Here, we are interested in computing ξ^2 , which in the

bosonic limit reads [46]

$$\xi_{N \rightarrow \infty}^2 = 1 + 2 \left(\langle \hat{b}^\dagger \hat{b} \rangle - |\langle \hat{b}^2 \rangle| \right). \quad (\text{E6})$$

Besides, to find a close e.o.m. for ξ we realize that, at the steady state, in the regime where $g_{\text{eff}} \ll 1$, Eq. (E5a) yields that the mean value of the cavity field coherence is a purely imaginary number, $\langle \hat{a} \rangle = -i2A/\kappa$. As a consequence, using Eq. (E5c) and Eq. (E5d), the mean value of the quadratic bosonic operator $\langle \hat{b}^2 \rangle$ is a real number. Thus, we can replace $|\langle \hat{b}^2 \rangle| \rightarrow \langle \hat{b}^2 \rangle$ in Eq. (E6). Taking the time derivative

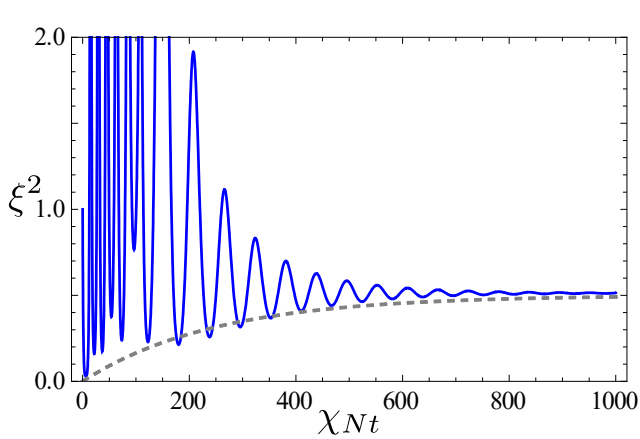


Figure 6. Full time dynamics for ξ^2 . The parameters used are $A = 10\kappa$ and $N g_{\text{eff}} = \kappa = \gamma = 1$

we arrive at Eq. (9) (see the main text), namely:

$$\frac{d\xi^2}{dt} = -(i4g_{\text{eff}}N\langle \hat{a} \rangle + \gamma)\xi^2 + \gamma. \quad (\text{E8})$$

In Fig. 6, we plot an example for the time dynamics of ξ^2 . Finally, in Fig. 7 we test the mean-field approximation comparing the system dynamics solved by numerical and analytical (using mean-field approximation) calculations. We compare both the mean number $\langle \hat{b}^\dagger \hat{b} \rangle$ and ξ^2 , finding a good agreement.

Finally, for completeness, let us explore the squeezing obtained in the limit $t \rightarrow \infty$ (stationary squeezing) setting the l.h.s of Eq. (E5a), Eq. (E5c) and Eq. (E5d) to zero. First, we introduce some dimensionless quantities, namely:

$$\mathcal{A}_\kappa := 2\mathcal{A}/\kappa, \quad \mathcal{G}_\gamma := 2N g_{\text{eff}}/\gamma, \quad \mathcal{G}_\kappa := 2N g_{\text{eff}}/\kappa. \quad (\text{E9})$$

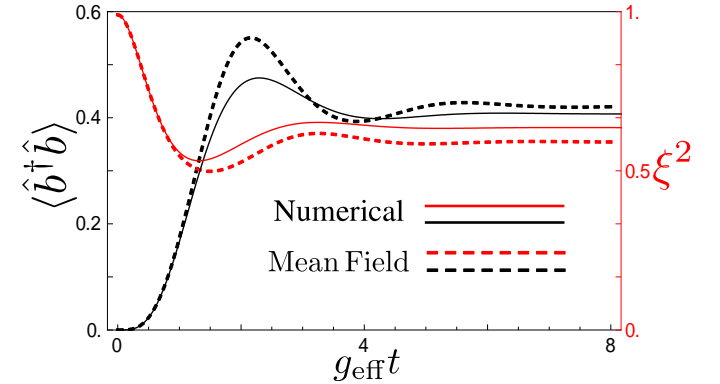


Figure 7. Comparison between the system dynamics solved by numerical calculations and using the mean-field approximation. We compare both the mean number $\langle \hat{b}^\dagger \hat{b} \rangle$ and ξ^2 . The parameters used are $\gamma = 5 \times 10^{-2} \omega_q$, $A = \gamma$, $\kappa = \gamma$ and $N g_{\text{eff}} = \kappa = \gamma = 1$.

From Eq. (E5c) and Eq. (E5d), we solve for $\langle \hat{b}^\dagger \hat{b} \rangle$ in the stationary state, obtaining

$$\langle \hat{b}^\dagger \hat{b} \rangle = \frac{2\mathcal{G}_\gamma^2 |\langle \hat{a} \rangle|^2}{1 - 4\mathcal{G}_\gamma^2 |\langle \hat{a} \rangle|^2}, \quad (\text{E10})$$

while using Eq. (E5a) and Eq. (E5c) we also get:

$$\langle \hat{a} \rangle = -i\mathcal{A}_\kappa + \mathcal{G}_\kappa \mathcal{G}_\gamma \langle \hat{a} \rangle (2\langle \hat{b}^\dagger \hat{b} \rangle + 1). \quad (\text{E11})$$

Combining Eq. (E10) with Eq. (E11) an equation for $\langle \hat{a} \rangle$ is obtained

$$\langle \hat{a} \rangle + \frac{\mathcal{G}_\kappa \mathcal{G}_\gamma \langle \hat{a} \rangle}{1 - 4\mathcal{G}_\gamma^2 |\langle \hat{a} \rangle|^2} = -i\mathcal{A}_\kappa \quad (\text{E12})$$

from which it follows that

$$\xi_{N \rightarrow \infty}^2 = 1 + 2(\langle \hat{b}^\dagger \hat{b} \rangle - |\langle \hat{b}^2 \rangle|) = \frac{1}{1 + 2\mathcal{G}_\gamma |\langle \hat{a} \rangle|} \quad (\text{E13})$$

The minimum of stationary squeezing is $\min(\xi_{N \rightarrow \infty}^2) = 1/2$. This can be understood by looking to Eq. (E11). There, it is easily checked that, when $\mathcal{A}_\kappa \rightarrow \infty$, then $1 - 4\mathcal{G}_\gamma^2|\langle \hat{a} \rangle|^2 \rightarrow 0$, thus $\xi_{N \rightarrow \infty}^2 \rightarrow 1/2$. The latter result has been verified numerically.